Magnetic behaviour of multisegmented FeCoCu/Cu electrodeposited nanowires

A Núñez[1,2], L Pérez[1,3], M Abuín[1,4], J P Araujo[5] and M P Proenca[5,6]

[1] Dept. Física de Materiales, Universidad Complutense de Madrid, 28040 Madrid, Spain
[2] Present address: Instituto de Microelectrónica de Barcelona, IMB-CNM (CSIC), Campus Universitat Autònoma de Barcelona, 08193 Bellaterra, Spain
[3] Instituto de Magnetismo Aplicado, UCM-CSIC-ADIF, 28230 Las Rozas, Madrid, Spain
[4] Present address: Deutsches Elektronen Synchrotron DESY, Notkestr. 85, 22607 Hamburg, Germany
[5] IFIMUP and IN - Institute of Nanoscience and Nanotechnology and Dep. Física e Astronomia, Univ. Porto, Rua do Campo Alegre 687, 4169-007 Porto, Portugal
[6] Instituto de Sistemas Optoelectrónicos y Microtecnología (ISOM), Universidad Politécnica de Madrid, Avda. Complutense 30, 28040 Madrid, Spain

E-mail: `marianapproenca@gmail.com`

Abstract. Understanding the magnetic behaviour of multisegmented nanowires (NWs) is a major key for the application of such structures in future devices. In this work, magnetic/non-magnetic arrays of FeCoCu/Cu multilayered NWs electrodeposited in nanoporous alumina templates are studied. Contrarily to most reports on multilayered NWs, the magnetic layer thickness was kept constant (30 nm) and only the non-magnetic layer thickness was changed (0 to 80 nm). This allowed us to tune the interwire and intrawire interactions between the magnetic layers in the NW array creating a three-dimensional (3D) magnetic system without the need to change the template characteristics. Magnetic hysteresis loops, measured with the applied field parallel and perpendicular to the NWs' long axis, showed the effect of the non-magnetic Cu layer on the overall magnetic properties of the NW arrays. In particular, introducing Cu layers along the magnetic NW axis creates domain wall pinning nucleation that facilitate the magnetization reversal of the wires, as seen by the decrease in the parallel coercivity and the reduction of the perpendicular saturation field. By further increasing the Cu layer thickness, the interactions between the magnetic segments, both along the NW axis and of neighbouring NWs, decrease, thus rising again the parallel coercivity and the perpendicular saturation field. This work shows how one can easily tune the parallel and perpendicular magnetic properties of a 3D magnetic layer system by adjusting the non-magnetic layer thickness.

1. Introduction

One-dimensional (1D) nanomaterials have been investigated during the past decades focusing on the miniaturization of devices. In particular, 1D nanowires (NWs) have attracted attention due to their application in novel fields such as biomedicine [1, 2], spintronics [3, 4] or multifunctional devices [5, 6]. For example, multisegmented NWs offer the possibility of using each magnetic domain as a storage bit [7, 8]. In addition, multisegmented NWs are a key component in the development of remote-controlled microbots [9, 10].

Template-filling by electrodeposition provides us with a unique method to fabricate multisegmented NWs with precise control of their diameter, interwire distance and length, as well as the thickness and composition of the different layers, thus creating versatile three-dimensional (3D) magnetic systems[11]. For this purpose, nanoporous polycarbonate or alumina membranes are used as templates in the electrodeposition process [12, 13]. In particular, in the past years, nanoporous alumina templates (NpATs) stood out as a popular method for the synthesis of various functional nanostructures. The use of these templates represents many advantages. It is a cheap method and easy to use and allows the synthesis of ordered NW arrays with precise control of diameter. When properly prepared, the pores self-organize in hexagonal pore arrangements, which also allows controlling the interpore distance [12].

Therefore, using a template process in the electrochemical deposition is an excellent method to grow NWs and enables the tuning of the composition and the morphology of multisegmented structures [14][15, 16, 17]. Segmented NWs with a magnetic/non-magnetic mutilayered structure grown by pulsed electrodeposition have been highly investigated in the last years: Co/Cu [18, 19, 20], Ni/Cu [21, 22, 23][24], Fe/Cu [25, 26], CoFeB/Cu [27], CoFe/Cu [28, 29, 30], CoNi/Cu [31, 14], CoPt/Pt [32], CoFe/Au [33], Ni/Au [34, 35], etc.. Most of these works aim the application of spin valves and the exploration of the giant magnetoresistance effect [36][37, 38]. Understanding the characteristics and magnetic behaviour of these 3D magnetic systems is necessary for devices application in the future.

In this work, pulsed electrodeposition was used to grow multisegmented NWs of FeCoCu/Cu inside hexagonally ordered nanoporous templates. The morphological, chemical, structural and magnetic characterization of the multisegmented $[FeCoCu/Cu]_{25}$ NW arrays is analysed as a function of the Cu layer thickness. This study allows us to better understand the influence of the Cu layer in the properties of these 3D magnetic systems aiming their application in future devices.

2. Experimental Details

Nanoporous alumina membranes were used as templates to grow multisegmented FeCoCu/Cu NWs. NpATs were fabricated by a two-step anodization process in a 0.3 M H_2SO_4 electrolyte at 4°C and a 25 V anodization potential. First and second

anodizations lasted 18 h and 40 h, respectively, leading to hexagonally ordered arrays of pores with interpore distances of ~ 65 nm, pores' diameter of ~ 30 nm and membrane thickness of ~ 150 μm. Chemical etching in an aqueous solution of 0.6 M $CuCl_2{\cdot}2H_2O$ and 1.2 M HCl is used to remove the remaining Al after anodization. Floating the membranes for 15 minutes in 0.5 M H_3PO_4 at 40°C removes the alumina barrier layer at the bottom of the pores. This last process enlarges the pores' diameter to 45 ± 5 nm. Finally, a thin Au layer of around 100 nm was evaporated at one side of the template to serve as the working electrode for the final electrodeposition of the NWs.

Electrodeposition was carried out in a three-electrode electrochemical cell with a single electrolyte solution and a potentiostat Ecochemie Autolab PGSTAT, using a Pt mesh as a counter electrode, an Ag/AgCl (BaSi) reference electrode and the NpATs with the previous Au evaporated layer as a working electrode. Before the electrodeposition of the NWs, the Au layer was thickened by electrodeposition. We used a commercial gold-plating solution (Orosene 999) and applied a potential of -1 V during approximately 5 min. Multisegmented FeCoCu/Cu NWs were then grown at room temperature by pulsed electrodeposition. Sulfate-based electrolytes were used, composed of 0.4 M H_3BO_3, 0.09 M $CoSO_4{\cdot}7H_2O$, 0.1 M $FeSO_4{\cdot}7H_2O$ and 0.005 M $CuSO_4{\cdot}5H_2O$. The pulsed electrodeposition method consisted on a pulse of -1.1 V to grow the FeCoCu alloy layer followed by a pulse of an optimized potential of -0.6 V to grow the Cu layer. In this work, multisegmented NWs formed by 25 bilayers of [FeCoCu/Cu] were electrodeposited. The Cu layer electrodeposition time was varied between 4 and 20 min, leading to layers of approximately 20 to 80 nm, while the FeCoCu alloy deposition time was kept constant (at 6 s), leading to ~ 30 nm of layer thickness. To better compare the structural and magnetic properties of the NW arrays, a sample without Cu segments (reference sample) was also fabricated by applying -1.1 V for 10 min.

3. Results and Discussion

3.1. Morphology and Composition

The morphology of the wires was analysed by scanning electron microscopy (SEM) using a FEI Inspect F50 microscope. In Fig. 1(a) a SEM image of a NpAT before any process was carried out to grow the NWs, is shown. The SEM image allowed us to verify the hexagonal order of the NpATs. Analysing this SEM image, diameters of ~ 45 nm and interpore distances of ~ 65 nm were determined. Figure 1(b) illustrates the quality of the electrodeposition process showing an uniform distribution of different magnetic and non-magnetic segments along the electrodeposited NWs. Total length of the NWs was ~ 3 μm. Moreover, closer analysis of the SEM images evidences the multilayered structure of the NWs with uniform layer length distributions. Figures 1(c) and (d) show the contrasting layers of different composition in the NWs. Detailed analysis of these images allowed us to measure the thickness of each layer. The results are summarized

in Table 1.

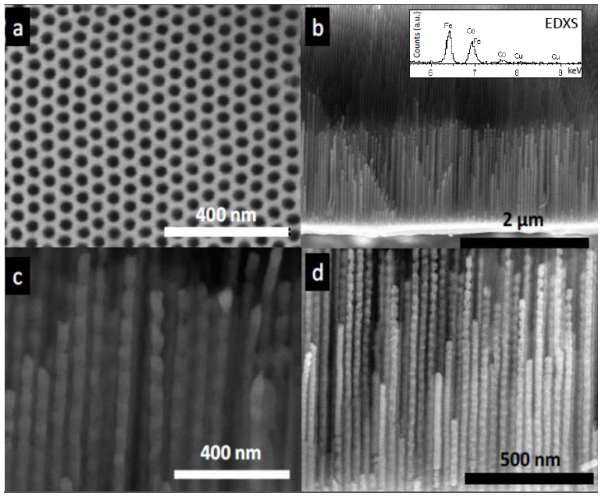

Figure 1. SEM images of different samples. (a) Bottom view of a NpAT before Au was deposited, illustrating the hexagonal oredered array of pores. (b) Template with multisegmented nanowires grown by pulse electrodeposition. Inset shows the EDXS spectrum of a FeCoCu alloy nanowire. (c) and (d) magnified view of the multisegmented nanowires, evidencing the different layers of FeCoCu/Cu electrodeposited.

Table 1. Structure of the studied multisegmented nanowires: the thickness of the CoFeCu layers is 30 nm and the final subscript indicates the number of layers of each component; δ_{Cu} is the Cu layer thickness. Magnetic characteristics of the multisegmented nanowires: coercive field (H_c), saturation field (H_{sat}) and reduced remanence (m_r), measured with the magnetic field applied parallel ($\parallel$) and perpendicular ($\perp$) to the nanowires' long axis.

Sample	δ_{Cu} (nm)	$H_c^{\parallel}$ (Oe)	$H_c^{\perp}$ (Oe)	$H_{sat}^{\perp}$ (Oe)	$m_r^{\parallel}$ (%)	$m_r^{\perp}$ (%)
(A1) FeCoCu(3000 nm)	0	660 ± 4	49 ± 1	4972 ± 80	18 ± 1	6 ± 1
(A2)[FeCoCu/Cu]$_{25}$	20 ± 4	430 ± 4	53 ± 1	3670 ± 25	16 ± 1	13 ± 1
(A3)[FeCoCu/Cu]$_{25}$	40 ± 6	353 ± 2	100 ± 3	2495 ± 55	19 ± 1	30 ± 1
(A4)[FeCoCu/Cu]$_{25}$	60 ± 10	330 ± 13	69 ± 2	2420 ± 110	11 ± 1	28 ± 1
(A5)[FeCoCu/Cu]$_{25}$	80 ± 10	795 ± 30	92 ± 5	3865 ± 755	43 ± 2	25 ± 3

Chemical composition was determined using an Oxford Instruments X-Max energy-dispersive X-ray spectrometer (EDXS). Inset in Fig. 1(b) shows the EDXS spectrum measured in the reference sample. This analysis of FeCoCu NWs reveals a composition of approximately 54% Fe, 43% Co and only 3% Cu. The relative Fe/Co ratio in the alloy is close to 1:1, ratio which is interesting in terms of the magnetic properties of the alloy (high saturation magnetization and low coercivity). In addition, the concentration

of Cu in the ferromagnetic alloy is very low. This agrees with previous assumptions that, when using low concentrations of Cu in the electrodeposicion solution, the amount of Cu that incorporate to the layers when applying the FeCo activation voltage is very small and do not significantly change the magnetic properties of FeCo alloys[21, 23].

3.2. Structural Characterization

The crystallographic structure of the FeCoCu alloy and Cu in the NWs was investigated using grazing incidence X-ray diffraction (GIXRD) with Panalytical X-ray diffractometers using Cu K_α radiation of $\lambda = 1.54056$ Å. Analysis of a FeCoCu electrodeposited NW array is shown in Fig. 2. This study confirms a body centred cubic (bcc) structure of FeCoCu alloy with a space group Pm3m. GIXRD patterns evidence three intensity peaks illustrating no preferred crystalline texture. No Cu peaks are shown in the XRD spectrum which agrees with EDXS analysis of only 3% concentration of Cu in the FeCoCu NWs. It is also worth to mention that no additional peaks corresponding to oxides are shown, nor peaks corresponding to metallic Co. GIXRD results allow to measure the lattice constant of the bcc structure, using the Bragg's law from the most intense peak value, $2\theta = 44.875°$. An experimental value of $a = 2.8541$ Å was obtained, which is smaller than the theoretical value of the FeCo alloy bcc lattice constant, $a = 2.8552$ Å. A reduction on the lattice constant by a 0.038% indicates that the bcc structure is tensioned. Inset in Fig. 2 evidences a shift of 0.6° in the intensity peaks due to the strain in the bcc system of the FeCoCu alloy. An explanation of this tensioned structure is that the Cu atoms are replacing the Fe or Co atoms in the alloy. Taking into account the atomic radius of the three elements, 135 pm for Cu, 140 pm for Fe and 135 pm for Co [39], we conclude that Fe atoms in the alloy are being replaced by atoms of Cu with smaller atomic radius, straining the crystal system [40]. Therefore, from a structural point of view, Cu atoms incorporate the structure of the FeCo alloy and the system grows as a FeCoCu Cu alloy [41, 42].

3.3. Magnetic Properties

A vibrating sample magnetometer (VSM), LakeShore Controller Model, 7304, allowed us to study the magnetic behaviour of the samples at room temperature. Magnetic hysteresis loops were measured using a saturation magnetic field of up to 10000 Oe. The magnetic field was applied both parallel and perpendicular to the NWs' long axis. Coercivity (H_c) and reduced remanence ($m_r \equiv M_r/M_{sat}$, where M_r and M_{sat} are the remanent and saturation magnetizations, respectively) were extracted from full hysteresis loops. Analysis of the magnetic hysteresis loops at a normalized magnetization of 0.9 allows to estimate the value of the saturation field (H_{sat}). Results are summarized in Table 1.

Figure 3 shows the magnetic hysteresis loops of selected samples (A1, A2 and A5). The elongated shape of these structures leads to a high aspect ratio (L/d, where L is the total length of the nanowires and d is the diameter), which causes a strong shape

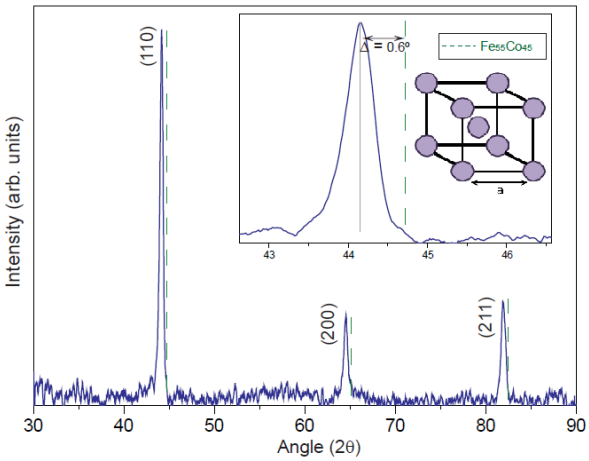

Figure 2. XRD spectrum of a $Fe_{54}Co_{43}Cu_3$ nanowire array with three intensity peaks of reflections (110), (200) and (211). Green-dashed lines indicate the peak positions of the theoretical $Fe_{55}Co_{45}$ system. Inset shows a shift of 0.6° in the results. A bcc crystal structure is also shown in the inset.

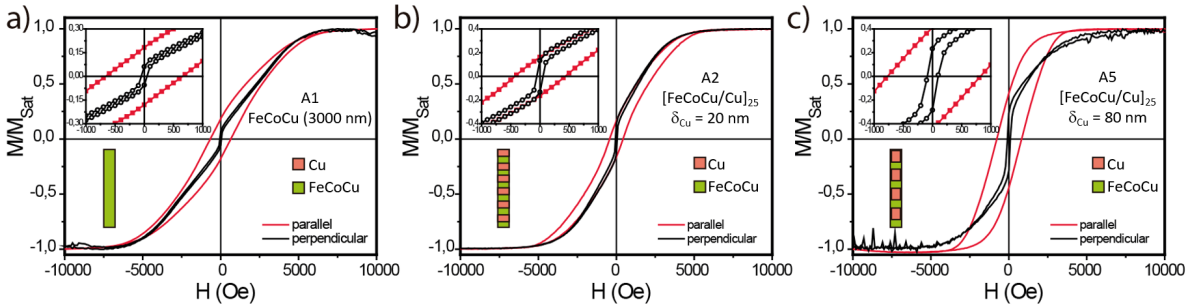

Figure 3. Magnetic hysteresis loops of samples (a) A1, (b) A2 and (c) A5, under parallel and perpendicular applied magnetic fields. Inset shows a detail of the hysteresis loops around zero applied field. The scheme of the morphology is also indicated.

anisotropy [31]. Therefore, all samples illustrate higher H_c values under parallel applied field, evidencing that the magnetic easy axis is lying along the NWs' long axis [2]. Another effect observed in Fig. 3 is the large tilt of the parallel magnetic hysteresis loops, which indicates the presence of strong magnetostatic interactions between the NWs in the array.

The most important results of the measured magnetic properties are illustrated in Fig. 4. A comparative study of all samples shows a characteristic magnetic behaviour when tuning the Cu layer thickness. Figure 4 illustrates the parallel coercivity ($H_c{}^{\parallel}$) and the perpendicular saturation field ($H_{sat}{}^{\perp}$) as a function of the Cu layer length of each sample.

Analysing the behaviour of the parallel coercivity in Fig. 4, a reduction of $H_c{}^{\parallel}$ is observed as the non-magnetic layer thickness increases. Samples A3 and A4, with 40 and 60 nm of Cu layer thickness, respectively, show the lowest values of $H_c^{\parallel}$. Introducing

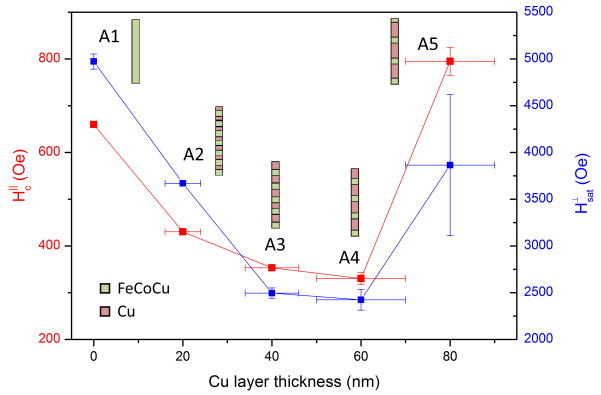

Figure 4. Coercivity values under parallel magnetic field as a function of Cu layer thickness (red). Saturation field values under perpendicular magnetic field as a function of Cu layer length (blue). Sample and scheme of the morphology are also indicated.

non-magnetic layers in the FeCoCu magnetic NWs generates nucleation points of new magnetic domain walls leading to an easier magnetization reversal, which explains the observed reduction of the $H_c{}^{\parallel}$ value from A1 to A4. This behavior was previously predicted by S. Allende et al. using Monte Carlo calculations[43].

Another contribution to the reduced value of $H_c{}^{\parallel}$ is the interaction between the FeCoCu alloy layers along the NW (intrawire interactions). Interactions between the magnetic layers facilitate the magnetization reversal along the NW, thus reducing the parallel coercive field. However, further increasing the Cu layer thickness (sample A5) decreases the number of domain wall nucleation sites and reduces the interaction between the magnetic layers, rising again the $H_c{}^{\parallel}$ value. This behaviour has also been recently observed in FeCoCu/Cu multisegmented NWs with longer magnetic segments using first-order reversal curve measurements [30]. It is important to note that $H_c{}^{\parallel}$ of sample A5 ($\delta_{Cu} \sim 80$ nm) takes a higher value than $H_c{}^{\parallel}$ of sample A1 ($\delta_{Cu} = 0$), concluding that the interactions between FeCoCu layers in sample A5 are very small. Under these conditions, the system behaves as a 3-dimensional array of non-interacting ferromagnetic $Fe_{54}Co_{43}Cu_3$ disks.

Moreover, Fig. 4 shows the saturation field as a function of the Cu layer thickness, evidencing a behaviour similar to the one observed for $H_c{}^{\parallel}$. Samples A3 and A4 exhibit again the lowest $H_{sat}{}^{\perp}$ values, concluding that introducing layers of Cu in the array also reduces the saturation field due to the nucleation points of new domain walls. When a perpendicular field is applied, all magnetic moments tend to align with it. Due to the small interwire distance (~ 20 nm), the magnetic layers of the array interact between neighboring NWs, reducing $H_{sat}{}^{\perp}$. Therefore, when a perpendicular magnetic field is applied, interwire interactions become dominant. The reduced $H_{sat}{}^{\perp}$ values obtained for samples A3 and A4, are thus due to the nucleation points of new domain walls and mainly the interaction of magnetic layers between neighbouring NWs, which facilitate the reversal mechanisms. Finally, in sample A5, the Cu layer thickness rises to 80 nm,

which reduces the magnetic interaction between neighbouring FeCoCu layers, increasing again the value of $H_{sat}{}^{\perp}$.

4. Conclusions

The magnetic properties of FeCoCu alloy NWs are influenced by the presence of a non-magnetic Cu layer. In this work, five samples of electrodeposited FeCoCu /Cu NW arrays with varying Cu layer thickness (from 0 to 80 nm), were studied. Morphology characterization confirmed the multilayer array of these structures with uniform layer thickness. Structural and chemical analysis verified the bcc FeCoCu alloy crystal structure and the segregation of Cu layers in the NW arrays. In all samples, a magnetic easy axis parallel to the NWs' long axis was confirmed. This work reported the changes in $H_c{}^{\parallel}$ and $H_{sat}{}^{\perp}$ of multisegmented magnetic/non-magnetic NW arrays with the non-magnetic layer thickness. Magnetic parameters are affected by the introduction of a multilayer array that generates the nucleation points of new domain walls. By applying a magnetic field along the NWs' long axis, one can tune the $H_c{}^{\parallel}$ values, as these are mainly affected by the interactions between magnetic layers along the NW axis (intrawire interactions). On the other hand, when a perpendicular field is applied, the interwire interactions (between magnetic layers of neighbouring NWs) become dominant, and one can tune the $H_{sat}{}^{\perp}$ values by adjusting the non-magnetic layer thickness. Concluding, changes in the electrodeposited Cu layer thickness allow one to tune the parallel and perpendicular magnetic properties of multisegmented NW arrays as desired, without the need to adjust the pore geometry of the template used.

Acknowledgments

The researchers involved in this work acknowledge financial support from FEDER and ON2 through project Norte-070124-FEDER-000070 and from FCT through the Associated Laboratory IN, project UID/NAN/50024/2013 and grant SFRH/BPD/84948/2012 (POPH/FSE). This work has been partially funded by MAT2014-52477-C5-1-P and MAT2014-52477-C5-2-P from the Spanish Ministerio de Ciencia e Innovación.

References

[1] Reich D H, Tanase M, Hultgren A, Bauer L A, Chen C S and Meyer G J 2003 *Journal of Applied Physics* **93** 7275–7280
[2] Ozkale B, Shamsudhin N, Chatzipirpiridis G, Hoop M, Gramm F, Chen X, Marti X, Sort J, Pellicer E and Pane S 2015 *ACS Applied Materials and Interfaces* **7** 7389–7396
[3] Fert A and Piraux L 1999 *Journal of Magnetism and Magnetic Materials* **200** 338–358
[4] Vandermeulen J, Van de Wiele B, Vansteenkiste A, Van Waeyenberge B and Dupré L 2015 *Journal of Physics D: Applied Physics* **48** 035001
[5] Liao L, Zhang Z, Yan B, Zheng Z, Bao Q L, Wu T, Li C M, Shen Z X, Zhang J X, Gong H, Li J C and Yu T 2009 *Nanotechnology* **20** 085203

[6] Martín-García L, Ruiz-Gómez S, Abuín M, Montaña Y, Carmona N and Pérez L 2015 *RSC Advances* **5** 97503–97507
[7] Atkinson D, Allwood D A, Xiong G, Cooke M D, Faulkner C C and Cowburn R P 2003 *Nature Materials* **2** 85–7
[8] Allwood D A A, Xiong G, Faulkner C C, Atkinson D, Petit D and Cowburn R P 2005 *Science* **309** 1688–92
[9] Kline T R, Paxton W F, Mallouk T E and Sen A 2005 *Angewandte Chemie* **117** 754–756
[10] Sanchez S, Solovev A A, Harazim S M and Schmidt O G 2011 *Journal of the American Chemical Society* **133** 701–703
[11] Ivanov Y P, Chuvilin A, Lopatin S and Kosel J 2016 *ACS nano* **10** 5326
[12] Sousa C T, Leitao D C, Proenca M P, Ventura J, Pereira A M and Araujo J P 2014 *Applied Physics Reviews* **1** 1–22
[13] Toimil-Molares M E 2012 *Beilstein Journal of Nanotechnology* **3** 860–83
[14] Qi K, Li X, Zhang H, Wang L, Xue D, Zhang H, Zhou B, Mellors N J and Peng Y 2012 *Nanotechnology* **23** 505707
[15] Cantu-Valle J, Díaz Barriga-Castro E, Vega V, García J, Mendoza-Reséndez R, Luna C, Manuel Prida V, Nielsch K, Mendoza-Santoyo F, Jose-Yacaman M and Ponce A 2015 *J. magn. magn. matter* **379** 294
[16] Garcia J, Vega V, Iglesias L, M Prida V, Hernando B, D Barriga Castro E, Medoza-resendez R, Luna C, Gorlitz D and Nielsch K 2014 *Phys. Status Solidi A* **211** 1042
[17] Zhang J, Salvador P, Sort J and Pellicer E 2016 *Adv. Mater. Interf.* **3** 1600336
[18] Liu K, Nagodawithana K, Searson P C and Chien C L 1995 *Physical Review B* **51** 7381–7384
[19] Fábián A, Terrier C, Guisan S S, Hoffer X, Dubey M, Gravier L, Ansermet J P and Wegrowe J E 2003 *Physical Review Letters* **91** 257209
[20] Reyes D, Biziere N, Warot-Fonrose B, Wade T and Gatel C 2016 *Nano Letters* **16** 1230–1236
[21] Chen M, Chien C L and Searson P C 2006 *Chemistry of Materials* **18** 1595–1601
[22] Maleak N, Potpattanapol P, Bao N, Ding J, Wongkokuo W, Tang I and Thongmee S 2014 *Journal of Magnetism and Magnetic Materials* **354** 262–266
[23] Susano M, Proenca M P, Moraes S, Sousa C T and Araújo J P 2016 *Nanotechnology* **27** 335301
[24] Carignan L P, Lacroix C, Ouimet A, Ciureanu M, Yelon A and Ménard D 2014 *J. Appl. Phys.* **102** 023905
[25] Dubois S, Chassaing E, Duvail J L, Piraux L and Waals M G 1999 *Journal De Chimie Physique Et De Physico-Chimie Biologique* **96** 1316–1331
[26] Almasi-Kashi M, Ramazani A, Kheyri F and Jafari-Khamse E 2014 *Materials Chemistry and Physics* **144** 230–234
[27] Akhtari-Zavareh A, Carignan L P, Yelon A, Ménard D, Kasama T, Herring R, Dunin-Borkowski R E, McCartney M R and Kavanagh K L 2014 *Journal of Applied Physics* **116** 023902
[28] Sahin T, Kockar H and Alper M 2015 *Journal of Magnetism and Magnetic Materials* **373** 128–131
[29] Ramazani A, Kashi M A, Eghbal F and Jafari-Khamse E 2015 *The European Physical Journal Plus* **130**
[30] Palmero E M, Béron F, Bran C, Real R P and Vázquez M 2016 *Nanotechnology* **27** 1–7
[31] Tang X T, Wang G C and Shima M 2007 *Journal of Magnetism and Magnetic Materials* **309** 188–196
[32] Peng Y, Cullis T, Luxmoore I and Inkson B 2011 *Nanotechnology* **22** 245709
[33] Park B C, Kim B G, Seo H W and Kim Y K 2014 *IEEE Transactions on Magnetics* **50** 2500204
[34] Clime L, Zhao S Y, Chen P, Normandin F, Roberge H and Veres T 2007 *Nanotechnology* **18** 435709
[35] Ishrat S, Maaz K, Lee K J, Jung M H and Kim G H 2014 *Journal of Solid State Chemistry* **210** 116–120
[36] Zhang W, Li H, Wang H and Yao S 2014 *Journal of The Electrochemical Society* **161** 176–180
[37] Bohnert T, Corinna-Niemann A, Michel A K, Babler S, Gooth J, Tóth B G, Neuróhr K, Péter L, Bakonyi I, Vega V, Prida V M and Nielsch K 2014 *Phys. Rev. B* **90** 165416

[38] Piraux L, George J M, Despres J F, Leroy C, Ferain E, Legras R, Ounadjela K and Fert A 1994 *Appl. Phys. Lett.* **65** 2484–2486
[39] Slater J C 1964 *The Journal of Chemical Physics* **41** 3199
[40] Garcia J, Prida V M, Vivas L G, Hernando B, Diaz Barriga Castro E, Mendoza R, Luna C, Escrig J and Vazquez M 2013 *Journal of Materials Chemistry C* **1** 3777
[41] Rodríguez-González B, Bran C, Warnatz T, Rivas J and Vazquez M 2014 *Journal of Applied Physics* **115** 133904
[42] Palmero E M, Bran C, Real R P, Magen C and Vazquez M 2014 *IEEE Magnetics Letters* **5** 6700304
[43] Allende S, Vargas N M, Altbir D, Vega, Gorlitz D and Nielsch K 2012 *Appl. Phys. Lett.* **101** 122412